Journal of Food Engineering 210 (2017) 27–34

Contents lists available at ScienceDirect

Journal of Food Engineering

journal homepage: www.elsevier.com/locate/jfoodeng

Application of non-enzymatic browning of fructose for heating pattern determination in microwave assisted thermal pasteurization system

Deepali Jain, Jungang Wang, Frank Liu, Juming Tang*, Stewart Bohnet

Biological Systems Engineering Department, Washington State University, Pullman, WA 99164, USA

ARTICLE INFO

Article history:
Received 6 October 2016
Received in revised form
31 March 2017
Accepted 10 April 2017
Available online 18 April 2017

Keywords:
Fructose degradation
Browning kinetics
Microwave pasteurization
Heating pattern
Dielectric properties

ABSTRACT

Various model foods and chemical markers have been used for the heating pattern determination in microwave processing at sterilization temperatures (110–130 °C). These chemical marker systems have slow reaction rates and are not useful at pasteurization temperatures (70–90 °C). In this study, non-enzymatic browning of fructose under alkaline conditions is investigated for its suitability to be used in the heating pattern determination for microwave assisted thermal pasteurization. Kinetics of browning of fructose in the mashed potato model food were studied. The model food samples were heated in a water bath at 60 °C, 70 °C, 80 °C and 90 °C for different time intervals and the browning kinetics were studied by spectrophotometric measurements at 420 nm. Reaction rate kinetics were fit to a linear first order kinetic model. Application of this model food to determine the heating pattern in the microwave assisted thermal pasteurization system was demonstrated. Dielectric properties of the mashed potato were measured to determine its suitability as a model food. Sucrose and salt were used as effective additives for the adjustment of the dielectric constants and loss factor respectively of the mashed potato. This system offers advantages of being cost-effective, opaque, homogeneous and easy to handle and thus provides an excellent system to locate the hot and cold spots of the food products.

1. Introduction

Introduction of the FDA Food Safety Modernization Act (FSMA), 2011 has increased academic and industry-wide interest in novel pasteurization technologies. In this regard, microwave processing is a promising thermal preservation technique for a variety of food products as it offers volumetric heating and short time exposure of high temperature (Tang, 2015).

A pilot-scale 915 MHz single mode microwave assisted pasteurization system (MAPS) has been developed at Washington State University that can be scaled up to process food products at 70–90 °C in food processing plants for control of bacterial and viral pathogens. The design of the system ensures repeatable and predictable heating patterns in pre-packaged foods.

Determination of the location of the cold spot is a critical step in developing process schedules in order to ensure food safety. Temperature sensors would have been the first choice to determine the heating patterns of the food processed by MAPS. However, implementation of sufficient numbers of sensors in moving food packages without altering the heating pattern in a microwave system is very challenging.

Kim et al. (1996) suggested using Maillard reaction products as chemical indicators of lethality for high-temperature short time processing. Proposed chemical markers M1(2,3-dihydro-3,5-dihydroxy-6-methyl-4(H)-pyran-4-one), M2(4-hydroxy-5-methyl-3(2H)-furanone) and M3(5-hydroxymethyl-furfural) are intermediate products of final brown pigment compounds produced due to the thermal processing of foods containing reducing sugars (Martins et al., 2000). However, it is a time-consuming process to study heating patterns in 3D food packages via quantitative measurement of marker yields using analytical methods. With advancements in digital imaging technology, a novel method based on the irreversible color change of the food during thermal processing was developed to visualize the intensity of heat treatment throughout the food package (Pandit et al., 2007). Heating patterns obtained by this technique (Pandit et al., 2006; Lau et al., 2003) are

* Corresponding author. Biological Systems Engineering, Washington State University, P.O. Box 646120, Pullman, WA 99164-6120, USA.
E-mail address: jtang@wsu.edu (J. Tang).

http://dx.doi.org/10.1016/j.jfoodeng.2017.04.014
0260-8774/

combined with single point temperature measurements and computer simulations (Chen et al., 2008, 2007; Resurreccion et al., 2013) to validate the temperature distribution and develop the processing schedule for microwave processing at sterilization temperatures (Luan et al., 2015b; Tang, 2015).

Model food systems developed for sterilization processes (110–130 °C) (Lau et al., 2003; Pandit et al., 2007; Ross, 1993; Ramaswamy et al., 1996; Wang et al., 2003) are not suitable for pasteurization (70–90 °C) applications due to the slower reaction kinetics. Previous research on development of model foods for pasteurization temperatures is very limited focusing only on Maillard reaction of ribose and lysine. A preliminary work conducted on the comparison of mashed potato, gellan gel and egg white gel model foods pointed out the limitations of egg white and gellan gel model food for heating pattern determination using image analysis (Bornhorst et al., 2017). The main limitations of these model foods are: high temperature (70 °C) exposure to form a gel, long preparation time and firm texture which is difficult to cut after processing. Therefore, a new model food system that is easy to prepare and cost-effective is required for the pasteurization temperature process.

Fructose is a reducing sugar which participates in Maillard reaction. It is known to undergo faster degradation reactions at higher pH of about 8–12 leading to faster browning rates (Ajandouz et al., 2001; Shaw et al., 1968) even without presence of amino acids (Shaw et al., 1968, 1971; Ledl et al., 1995). Fructose in alkaline conditions undergoes an equilibrium via 1,2 and 2,3-enediol anion species, known as Lobry de Brujn-Alberda van Ekenstein rearrangement. The enediol intermediate undergoes non-reversible degradation reactions, including β elimination, benzylic-acid rearrangements and aldol condensation reactions, with subsequent formation of brown pigments (Eggleston and Vercellotti, 2000).

Thus, the objectives of this study were: (i) to investigate the formation of brown pigments via fructose degradation under pasteurization conditions in order to correlate the color change with intensity of thermal processing; (ii) to validate the application of the new model system in heating pattern evaluation of the MAPS process using computer vision method; and (iii) to adjust dielectric properties of the new model food to match a wide range of food products.

2. Materials and methods

2.1. Food preparation and thermal treatment

Mashed potato model food was prepared by mixing 20% (w/w) dry potato flakes (Oregon Potato Company, WA) and 1.8% fructose in 1 M sodium hydroxide solution. 1.5 g of model food was heated at 60 °C, 70 °C, 80 °C and 90 °C in thermal cells described in Zhang et al. (2014). The come-up time (CUT), defined as the time for the coldest spot in the sample to reach within 0.5 °of the target, was measured to be 1.5–2 min using a calibrated type-T thermocouple. After heating samples were taken out at the intervals of 2, 5, 10, 15 and 20 min and were cooled down using an ice bath to stop the further reaction. The heating time of the sample was measured excluding CUT. After heating, model food samples were mixed in 10 ml of water and centrifuged for 10 min at 8000 rpm. The supernatant was used for further measurements. For dielectric properties measurement, salt and sugar were added to the water along with fructose and sodium hydroxide followed by mixing in the dried potato flakes. The initial pH of the model food was measured to be 11 which was not affected by the addition of salt or sucrose. All the experiments were conducted in triplicates.

2.2. UV absorbance and browning

UV–vis measurement was performed using a Pharmacia Biotech (Cambridge, England) Ultrospec 4000 spectrophotometer. Brandtech disposable UV-transparent Cuvettes were used. Appropriate dilutions were made in order to obtain absorbance values less than 1.5. Absorbance values at 420 nm were used as indicator of brown color development during the reaction (Ajandouz et al., 2001). Readings were multiplied by the dilution factor for further analysis.

2.3. Modelling procedure

It is known that any reagent or chemical reaction which follows an nth order kinetics with a rate constant that follows the Arrhenious equation can be used for mapping heating uniformity in thermal processing (Ramaswamy et al., 1996; Hendrickx et al., 1992). Thus, experimental data obtained by spectrophotometric measurements at 420 nm was fitted to the following reaction kinetics equation as described by previous researchers (Kim et al., 1996; Pandit et al., 2007).

$$\frac{\mathrm{dM}}{\mathrm{d}t} = k[T(t)](M - M_\infty)^n \tag{1}$$

where M is absorbance at time t, M_∞ is the absorbance at saturation and k is the rate constant at the processing temperature. M_∞ is defined as the point after which there is no effect of further heating on the browning intensity. To obtain the saturation color absorbance value (M_∞), samples were heated for 60 min at 60, 70, 80 and 90 °C. and then treated in the same manner as described above. For the fructose browning reaction, ($n = 0$) zero order and ($n = 1$) first order kinetics fit was evaluated using Minitab 12. Statistical parameters of regression (R^2 and S) were obtained directly from the software. The standard error of regression (S) value represents the average deviation of the experimental data from the regression line. It must be <= 2.5 to produce a sufficiently narrow 95% prediction interval. The lower the value of S, the more precise is the regression. For zero order, Equation (1) has the solution of the form:

$$M(t) = kt \tag{2}$$

A first order differential equation (Kim et al., 1996; Ross, 1993) has the solution of the form

$$M(t) = M_\infty\left[1 - e^{-kt}\right] \tag{3}$$

Plotting of log[1−M/M_∞] vs time gives a straight line with a slope equal to the first order rate constant.

2.4. Food properties measurement

In microwave heating, dielectric properties are principal parameters which determine how the energy is absorbed and distributed inside a food material and hence can affect the heating pattern (Tang and Resurreccion, 2009). Dielectric properties are described by complex relative permittivity (ε_r^*) which has two components: relative dielectric constant (ε_r') and relative dielectric loss factor (ε_r'').

$$\varepsilon_r^* = \varepsilon_r' - j\varepsilon_r'' \tag{4}$$

where $j = \sqrt{-1}$. The dielectric constant reflects the energy storage capability when electromagnetic energy is incident on the material, and the loss factor is associated with the conversion of electromagnetic energy into thermal energy used for heating the food (Wang et al., 2003). The effect of salt on dielectric properties at

0.58%, 1.2% and 1.8% and sucrose at 0.2 g/ml and 0.3 g/ml concentration was studied. The criteria for choosing salt levels was based on the recommended levels in MAPS processing to obtain the optimum penetration depth (Guan et al., 2004; Zhang et al., 2015). The dielectric constant is mainly a function of water content (Luan et al., 2015a; Zhang et al., 2015). Therefore the purpose of adding 0.2 g/ml and 0.3 g/ml sucrose was to reduce the water content to 60% and 50%, respectively.

Dielectric properties were measured using an HP 8752 C Network Analyzer and 85070B Open-End Coaxial Dielectric Probe (Agilent Technologies, Santa Clara, CA) in the microwave frequency range: 0.3–3 GHz. The measurements were carried out at temperatures of 25 °C, 30 °C, 40 °C, 50 °C, 60 °C, 70 °C, 80 °C, 90 °C, and 100 °C. All measurements were conducted in triplicate.

2.5. Microwave assisted thermal pasteurization (MAPS) processing

A pilot scale MAPS system has four sections: preheating, microwave heating, holding and cooling. The microwave heating section consists of two rectangular cavities connected to a 915 MHz generator. The details of the design of the single mode cavities for the heating section is described by Tang (2015).

For processing, the food samples were added to 16 oz trays (160 mm × 125 mm × 16 mm), vacuum sealed and kept at 4 °C overnight for MAPS treatment. The trays were placed on a patent pending carrier and moved horizontally inside the cavities. The preheating water, circulating water in the cavities, holding section and cooling temperature were set at 61 °C, 93 °C, 93 °C and 23 °C, respectively. Food in 16 oz trays was pre-heated for 30 min, heated in the microwave section with a residence time of 2.8 min, and then the food trays were moved to the holding section for 5 min. The samples were cooled down in the cooling section for 5 min and unloaded.

2.6. Heating pattern determination by computer vision assistant

After processing, the mashed potato model food was kept at 4 °C overnight. Due to the symmetrical design of the MAPS system, the vertical location of the cold spot is in the middle layer of the food (Zhang et al., 2014). The location of the cold spot in the middle layer was also validated by temperature measurements and computer simulations (Resurreccion, 2012; Luan et al., 2015b). Therefore the food was cut horizontally in half and the images were taken using a camera set-up described previously by Pandit et al. (2007). The analysis of the images was done using Adobe Photoshop with the computer vision assistant technique (Pandit et al., 2006). The software divided the whole food sample image into various grids and based on the lowest and highest color values, the exact location of the cold and hot spot was determined. The software converted the most heated parts of the processed model food to red color (hot spots) and the least heated to blue color (cold spot). Areas which received a medium amount of thermal energy were converted to other colors between blue and red. All experiments were performed in duplicate.

2.7. Temperature profile

To validate the location of cold and hot spots determined by the browning reaction, PICO-VACQ 1Tc mobile metallic temperature sensors manufactured by TMI-Orion (Castelnau-le-Lez, France) were used as shown in Fig. 1. Presence of metal temperature sensors in a food package could create high temperature zones near the tip of the sensors, caused by interaction of the electric field with the probe tip. Therefore sensors with a spherical tip placed perpendicular to the dominant electric field component (E_y) were used to reduce the distortion of electric fields (Luan et al., 2015b), as shown in Fig. 2.

The trays were filled with 454 g of mashed potato model food and vacuum-sealed (100 mbar) with lid film (sealing conditions: 200 °C for 4 s dwell time) and a vacuum sealer (Multivac T-200, Multivac Inc., Kansas City, MO, U.S.A.). Samples were processed using 7 KW total microwave power and a tray speed of 13.5 mm/s. This speed provided 2 min of microwave heating. The microwave heating was followed by hot water heating in the holding section for 10 min at 90 °C. The process was designed to achieve a desired lethality for a 6 log reduction of psychrotrophic non-proteolytic *Clostridium botulinum* spores type B and E ($P_{90°C} = 10$ min) at the cold spot (ECFF, 2006). Finally, all the trays were cooled in the cooling section at 23 °C. Sensors were taken out after processing and the data were recorded. The cumulative lethality (P) was calculated using the following equation:

$$P = \int_0^t 10^{(T-T_{ref})/z} dt \quad (5)$$

where T_{ref} is 90 °C and z value is 9.84 °C for *C. botulinum* type B & E.

3. Results and discussion

3.1. Browning kinetics

The absorbance values at 420 nm in Fig. 3 show that in general browning increased with time and temperature. The browning at 60 °C and 70 °C increases almost linearly with time (zero order $R^2 = 0.98$). However at 80 °C and 90 °C exponential behaviour is observed. Table 1 shows zero order and first order rate constants

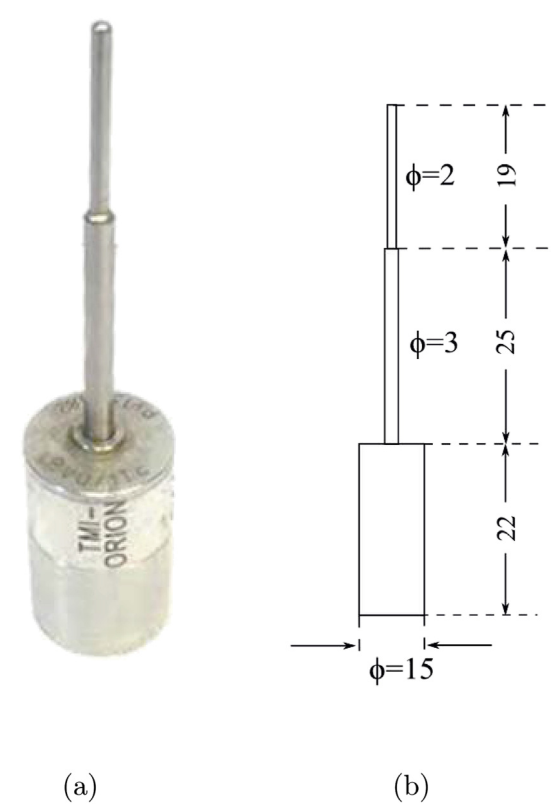

Fig. 1. (a) Mobile metallic sensor for temperature measurement in moving trays inside microwave assisted thermal pasteurization system and (b) its dimensions (in mm).

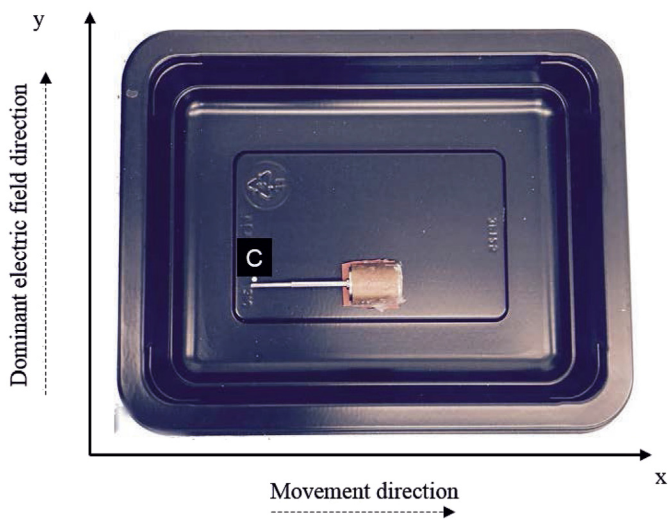

Fig. 2. Temperature sensor placed at the cold spot location in the 16 oz sample tray: The tray with the sensor was filled with 454 g of model food and vacuum packaged followed by MAPS processing for the lethality measurement.

with regression coefficients. At all temperatures accuracy (R^2 value) of the first order model was either better or equal to the zero order kinetics. Therefore, first order rate constants were considered for further analysis.

Fig. 4 shows first order (Equation (3)) fit to brown color development in the process of fructose degradation at 60 °C, 70 °C, 80 °C, and 90 °C. S value of 0.035, 0.037, 0.102 and 0.408 were obtained at 60 °C, 70 °C, 80 °C, and 90 °C, respectively. In all cases, S values were much less than 2.5%, which shows the accuracy of fitting to the linear model.

Temperature dependence of the rate constant of browning reaction was fitted to Arrhenius type equation with a R^2 value of 0.98, giving activation energy (E_a) of 76.6 kJ/mol (Fig. 5). This value matches with the range reported in the literature for non-enzymatic browning in fruits and vegetables (16–30 kcal/mol)(-Labuza and Baisier, 1992). The activation energy of browning obtained in this work is in the range of activation energies cited for

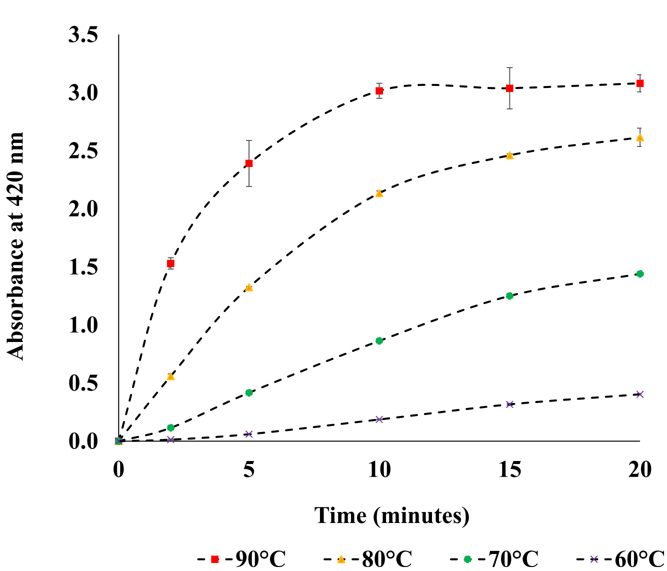

Fig. 3. Absorbance at 420 nm (Brown color development) measured in the model food heated at 60 (×), 70(●), 80(▲) and 90 (■) °C for different time intervals (2–20 min).

Table 1
Reaction rate constants for color change of fructose under alkaline conditions obtained from zero order and first order log linear model fit to absorbance at 420 nm at 60 °C, 70 °C, 80 °C and 90 °C.

T(°C)	Zero order K_{max} (min^{-1})	R^2	1st order K_{max} (min^{-1})	R^2
60	0.020	0.98	0.030	0.98
70	0.077	0.98	0.041	0.99
80	0.160	0.83	0.102	0.99
90	0.129	0.68	0.291	0.98

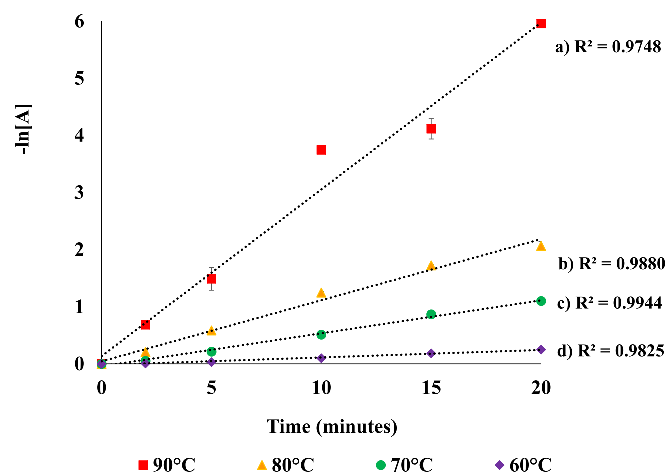

Fig. 4. First order model fit to color change kinetics of fructose in mashed potato model food at different temperature; $A = [1 - M/M_\infty]$, M is absorbance at time t, M_∞ is saturation absorbance at a) 90 °C (■) b) 80 °C (▲) c) 70 °C ● d) 60 °C (♦). (For interpretation of the references to colour in this figure legend, the reader is referred to the web version of this article.)

chemical markers used in microwave processing. A range of 81.4–96.1 kJ/mol for chemical marker M2 in mashed potato model food (Pandit et al., 2006) and 81.5 kJ/mol in whey protein gels (Lau et al., 2003) have been reported in the literature. Wang et al. (2004) reported activation energy of M1 formation in whey protein gel and broccoli extract in the range of 85.6–120.9 kJ/mol.

3.2. Color and lethality correlation

Plots of calculated lethality versus experimental absorbance

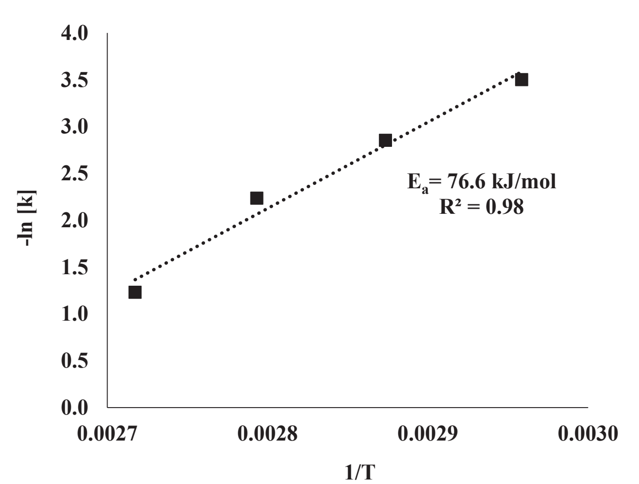

Fig. 5. Temperature (T, K) dependence of first order rate constant (k, min^{-1}) of browning reaction of fructose described by Arrhenius relationship.

values obtained at 60, 70, 80, and 90 °C are shown in Fig. 6. Lethality was calculated using Equation (5). R^2 > 0.97 at all temperature shows a significant linear relationship between browning and lethality. Positive correlation suggests that lower lethality was achieved at lower absorbance value. Therefore, it can be deduced that areas with lower concentration of brown pigments had received lower amounts of thermal energy and vice versa.

3.3. Dielectric properties of model food

MAPS is designed to process food products such as vegetables, fruits, pasta, meat and dessert, which have a broad range of dielectric properties (Wang et al., 2003, 2008; Peng et al., 2014). It is essential for model foods to have matching dielectric properties with food products in order to evaluate and validate the temperature distribution within the foods.

Figs. 7 and 8 show the dielectric constant and loss factor of model food changing with temperature and frequency. The dielectric constant of the mashed potato model food decreased with temperature as well as frequency. The decline of the constant was more at higher temperatures (>70 °C). The effect of frequency and temperature on the loss factor is more complex: the dielectric loss factor increased with temperature upto 1.2 GHz. For frequencies in the range of 1.2–2.1 GHz, a slight increase was observed for temperatures between 50–100 °C. At higher frequencies (2.1–3 GHz) no significant difference was observed in the loss factor at all temperatures. A similar trend of dielectric properties of food has been reported by many researchers in the past (Guan et al., 2004; Luan et al., 2015b; Zhang et al., 2015). This phenomenon is attributed due to the two types of contribution to loss factor i.e. ionic and dipolar. Ionic dielectric loss factor has a linear relationship with conductivity and frequency, and dominates at lower frequencies. However, the dipole contribution due to polarization of the water molecules dominates at the higher frequencies (Tang,

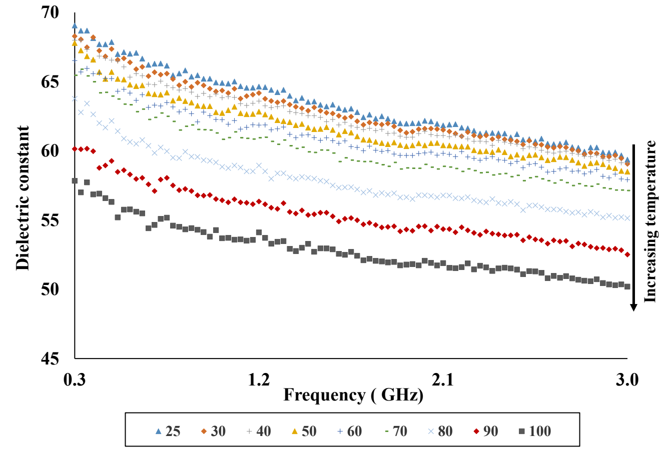

Fig. 7. Effect of temperature on dielectric constant of mashed potatoes model food in the frequency range of 0.3–3 GHz.

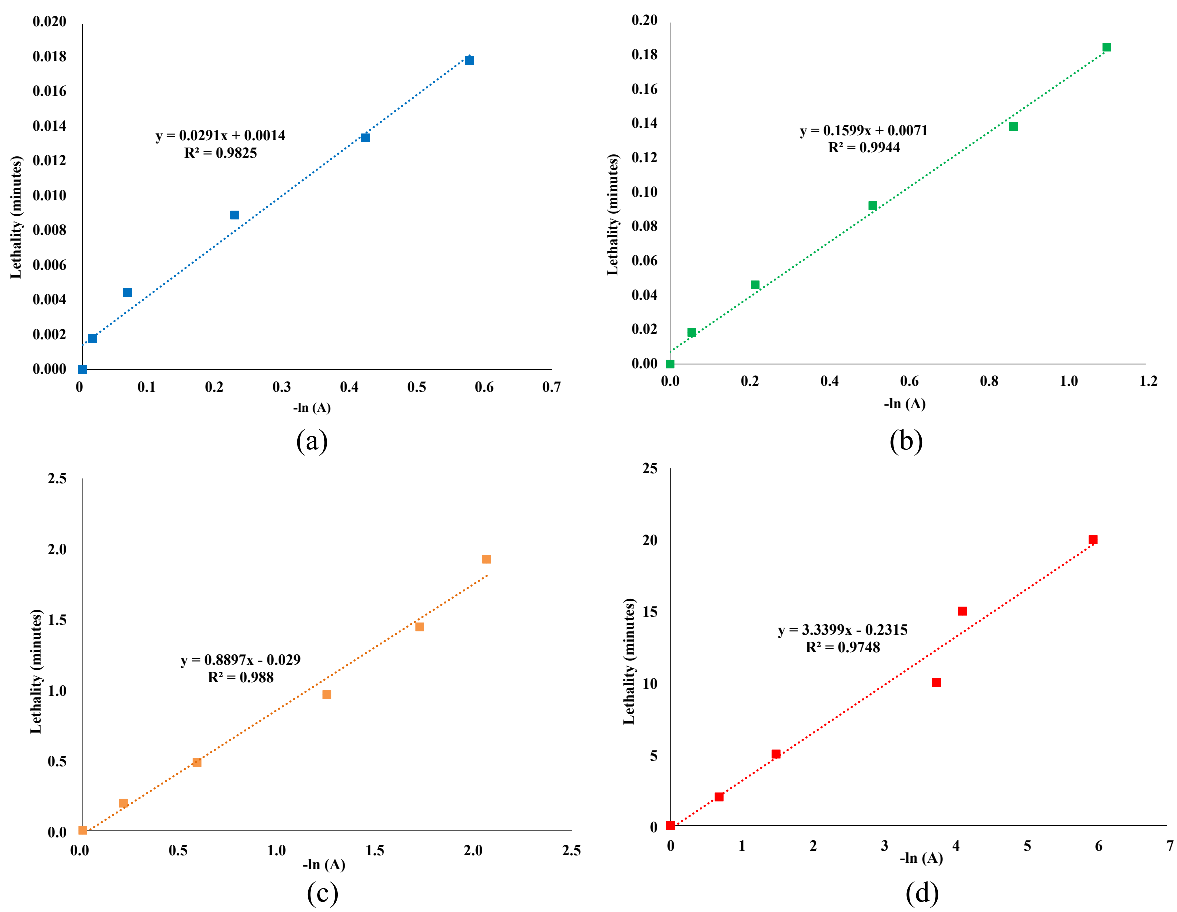

Fig. 6. Calculated lethality of *Clostridium botulinium* type E as a function of experimental color change measured by spectrophotometric absorbance at 420 nm at (a) 60 °C (■) (b) 70 °C (■) (c) 80 °C (■) and (d) 90 °C (■). Linear regression coefficients and equations are shown for each model (- - -). (For interpretation of the references to colour in this figure legend, the reader is referred to the web version of this article.)

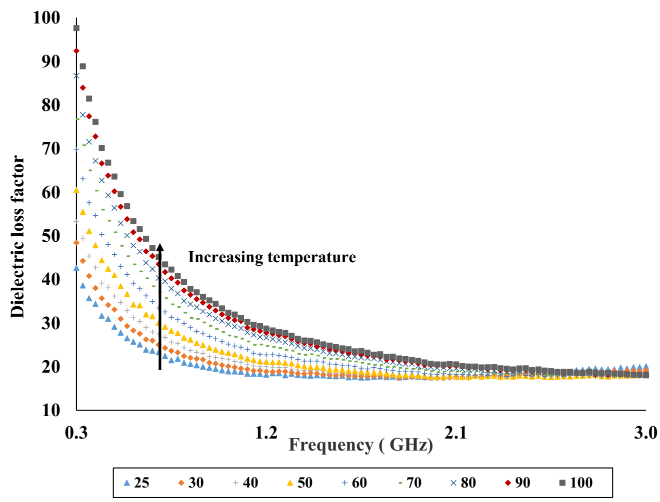

Fig. 8. Effect of temperature on dielectric loss factor of mashed potatoes model food in the frequency range of 0.3–3 GHz.

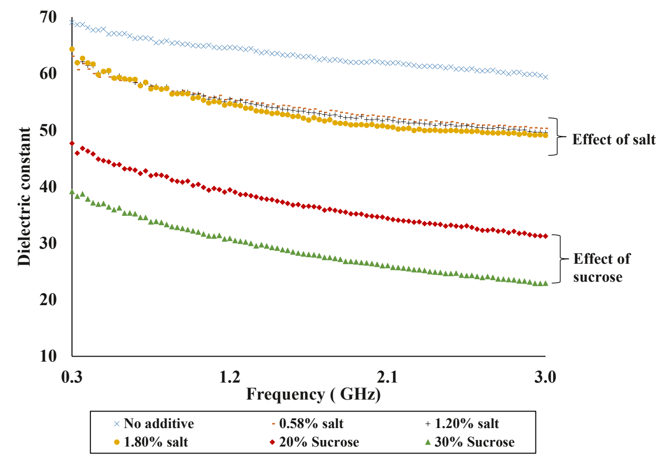

Fig. 9. Effect of 30% (▲) and 20% (♦) sucrose and 0.58% (▬), 1.2% (+), 1.8% (●) salt addition on dielectric constant of model food at 25 °C in the frequency range of 0.3–3 GHz; Dielectric constant data of model food without additive is shown (×).

2015; Zhang et al., 2015). Dielectric constant and loss factor values at 915 MHz obtained at the measured temperature range is listed in Table 2.

The effect of salt and sucrose addition on the dielectric constant and loss factor of the model food in the frequency range 0.3–3 GHz at 25 °C are shown in Figs. 9 and 10, respectively. The presence of 0.56% salt reduced the value of ε' from 63.1 to 56 at 915 MHz but it did not change further by increasing the salt concentration to 1.2 and 1.8%. A significant decrease in the dielectric constant (at 915 MHz and 25 °C) from 63.1 to 40 and 32 was observed by the addition of sucrose at 20% and 30% respectively. This effect could have been caused by the lower amount of water content in the model food or due to the binding of sugar-water molecules. As shown in Fig. 10, addition of 20% sucrose did not have any effect on the loss factor; but when adding 30% sucrose, ε'' decreased slightly. This could be either due to the lower amount of water or an increase in the viscosity of the sample which reduced the ion mobility. Increasing salt amount in the food increases the loss factor (at 915 MHz and 25 °C) from 17 at 0% to 28, 40, and 47 at 0.56%, 1.2% and 1.8% respectively. This increase is attributed to the conduction contribution of the loss factor. These values are similar to those reported by Guan et al. (2004) in their studies for mashed potatoes. An increase in salt content from 0.8% to 2.8% in mashed potatoes caused a slight increase in the dielectric constant from 64 to 62, but increased the loss factor from 27.1 to 52.4, at 915 MHz and 20 °C (Guan et al., 2004). Slightly lower values of the loss factor obtained in this work is due to the different amount of salt content used in the preparation.

Table 2
Dielectric properties (dielectric constant ε' and loss factor ε'') of mashed potato model food in temperature range 25°C–100 °C at 915 MHz.

T(°C)	ε'	ε''
25	63.1 ± 2.0	19.1 ± 0.9
30	62.4 ± 2.1	20.5 ± 1.2
40	61.6 ± 2.4	21.8 ± 0.8
50	61.1 ± 2.1	23.8 ± 0.9
60	60.5 ± 1.7	26.4 ± 1.0
70	59.9 ± 1.4	29.2 ± 0.5
80	58.4 ± 0.5	32.1 ± 0.1
90	56.9 ± 0.2	34.1 ± 0.3
100	54.8 ± 1.0	35.8 ± 0.2

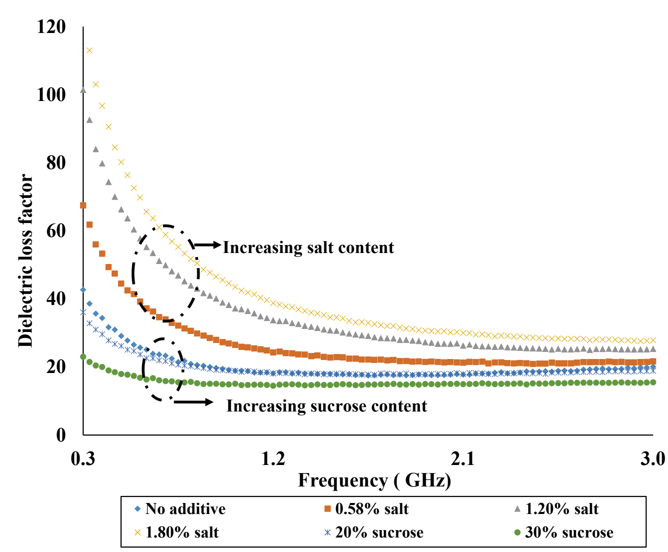

Fig. 10. Effect of 30% (●) and 20% (✳) sucrose and 0.58% (■), 1.2% (▲), 1.8% (×) salt addition on dielectric loss factor of model food at 25 °C in the frequency range of 0.3–3 GHz; Dielectric loss factor of model food without additive is shown (♦).

3.4. Application of the mashed potato model food in MAPS processing

A clear heating pattern in 16 oz trays based on browning of mashed potato model food after processing in microwave assistant pasteurization system was obtained. Four symmetrically located hot zones (areas which received the highest amount of thermal energy) and two cold zones (which received the lowest amount of thermal energy) (Fig. 11) were observed. Fig. 12 shows the location of cold and hot spots detected by the computer vision method. In order to validate results of the computer vision method for the new model system for the MAPS process, samples from the middle layer of the processed food from point 1, 2, 3, 4, 5 and 6 were taken and the absorbance was recorded. Fig. 13 shows the absorbance at 420 nm taken at locations 1, 2, 3, 4, 5 and 6. Absorbance at locations 1, 2, 3 and 4 are higher than the absorbance at locations 5 and 6. This finding confirms the result of the computer vision assistant method that locations 1, 2, 3 and 4 received higher thermal energy than the locations 5 and 6. Among hot spots, the number 1 location

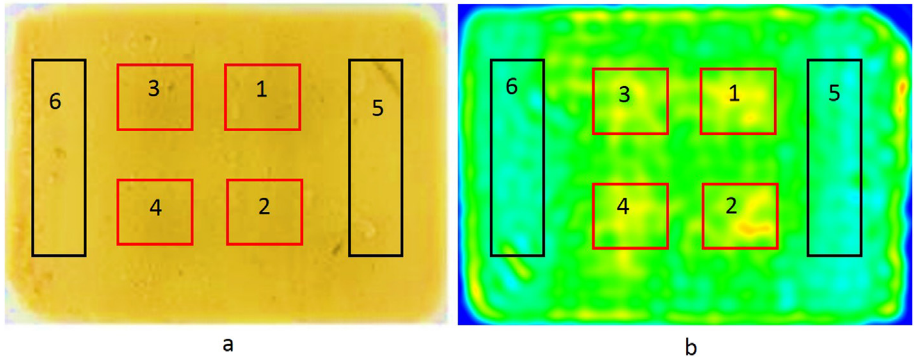

Fig. 11. Heating pattern of middle layer of model food filled in 16 oz trays obtained after microwave processing in MAPS a) Brown color development in mashed potato model food b) after computer vision assistant analysis; red areas represent hot spots and blue areas are cold spot. (For interpretation of the references to colour in this figure legend, the reader is referred to the web version of this article.)

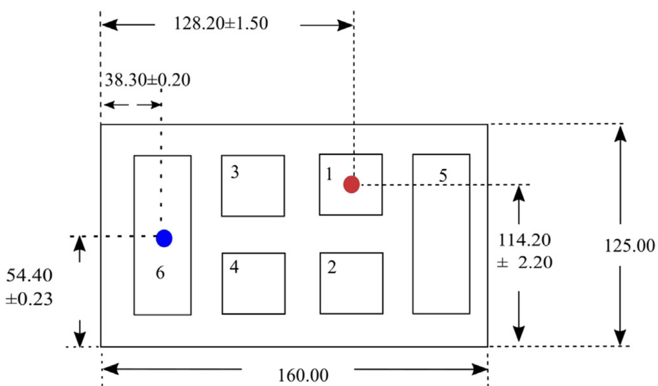

Fig. 12. Location of cold (blue colored circle) and hot (red colored circle) spots in 16 oz trays determined by computer vision assistant analysis; dimensions in mm. (For interpretation of the references to colour in this figure legend, the reader is referred to the web version of this article.)

gave the highest browning value whereas for the cold spot, location 6 gave the lowest.

Temperature profiles at the hot (location 1) and cold (location 6) spots were recorded using mobile metallic temperature sensors. The sensors were installed in a metallic protective tube and a rubber cushion was used to set the height of the tip at the middle layer of the food. The sensor was fixed in the middle layer so that the tip is located at the predetermined hot and cold spots locations. The temperature at the hot spot was always higher than the temperature at the cold spot. This ensures the reliability of the computer vision method for the accurate determination of hot and cold spots in this new model food during MAPS processing at 90 °C.

Fig. 14 shows a time temperature profile obtained in MAPS system using temperature sensors installed at the hot and cold spots. However, converting absorbance values quantitatively predicted lethality (P_{90}) of 6 and 3.5 min at the hot and cold spots, respectively, which was lower than the temperature sensor measurements. The possible reason for this discrepancy was that the model food was kept overnight in refrigeration for easy cutting. That might have led to the diffusion of pigments from higher concentration areas to lower concentration. Similar stability challenge was observed for the chemical marker M2 concentration in egg white model food (Zhang et al., 2014) and M1 formation in meat beads (Ramaswamy et al., 1996). Small time gap between processing and evaluation of the absorbance will help in reducing the estimation errors. In view of these possible experimental errors, we believe that further calibration of the model food is required for the exact quantitative calculation of lethality using brown

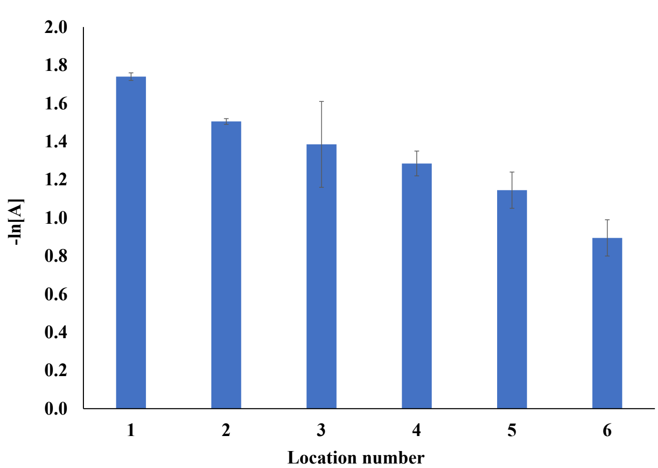

Fig. 13. Absorbance values at 420 nm for different hot spots (1, 2, 3 and 4) and cold spot (5 and 6) locations in mashed potato model food after MAPS processing at 90 °C.

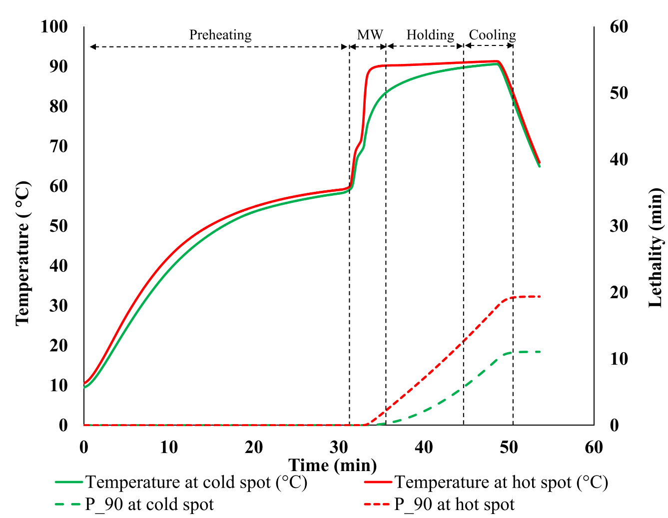

Fig. 14. Temperature profiles and accumulated lethality measured using temperature sensors located at hot (▬) and cold(▬) spots determined by computer vision assistant method by analysing browning of the mashed potato model food. Primary y axis represent temperature (solid lines) and secondary y axis is lethality (dashed lines) calculated for *Clostridium botulinium* type E.

pigments. However this model system can successfully be used to map the intensity of heating received by the food and determine the locations of the hot and cold spots, where there are no viable alternatives available.

4. Conclusion

In this paper, the non-enzymatic browning of fructose and its applicability to the determination of heating patterns of the microwave assisted thermal pasteurization process was evaluated. First order log linear kinetics was used to describe the color change in mashed potato model food with time and temperature, and first order rate constant showed Arrhenius type temperature dependence. Addition of salt and sucrose was used to adjust the dielectric loss factor and constant of the food, respectively. This model food in combination with single point temperature measurements will be used to predict and evaluate the heating patterns and develop the processing schedules for a wide variety of food products. It would also serve as a heating pattern validation tool for a computer simulation model of the MAPS system.

Acknowledgments

Authors would like to thank USDA Agricultural and Food Research Initiative 444 (AFRI) CAP grant 2016-68003-23415 to support this study.

References

Ajandouz, E., Tchiakpe, L., Dalle Ore, F., Benajiba, A., Puigserver, A., 2001. Effects of pH on caramelization and maillard reaction kinetics in fructose-lysine model systems. Food Chem. 66 (7), 926–931.

Bornhorst, E.R., Tang, J., Sablani, S.S., Barbosa-c, G.V., 2017. LWT - food Science and Technology Development of model food systems for thermal pasteurization applications based on Maillard reaction products novas. LWT–Food Sci. Technol. 75, 417–424.

Chen, H., Tang, J., Liu, F., 2007. Coupled simulation of an electromagnetic heating process using the finite difference time domain method. J. Microw. Power Electromagn. Energy 41 (3), 50.

Chen, H., Tang, J., Liu, F., 2008. Simulation model for moving food packages in microwave heating processes using conformal FDTD method. J. Food Eng. 88 (3), 294–305.

Eggleston, G., Vercellotti, J.R., 2000. Degradation of sucrose, glucose and fructose in concentrated aqueous solutions under constant ph conditions at elevated temperature. J. Carbohydr. Chem. 19 (9), 1305–1318.

European Chilled Food Federation (ECFF), 2006. Recommendations for the Production of Prepackaged Chilled Food, second ed. European Chilled Food Federation.

Guan, D., Cheng, M., Wang, Y., Tang, J., 2004. Dielectric properties of mashed potatoes relevant to microwave and radio-frequency pasteurization and sterilization processes. Food Eng. Phys. Prop. 69 (1).

Hendrickx, M.E., Weng, Z., Maesmans, G., Tobback, P., 1992. Validation of a time-temperature integrator for thermal processing of foods under pasteurization conditions. Int. J. Food Sci. Technol. 27, 21–31.

Kim, H.-J., Taub, I.A., Choi, Y.-M., Anuradha, P., 1996. Principles and applications of chemical markers of sterility in high temperature Short time processing of particulate foods. In: Lee, T.-C., Kim, H.-J. (Eds.), Chemical Markers for Processed and Stored Foods, first ed. American Chemical Society, Rutgers, pp. 54–69 (chapter 6).

Labuza, T.P., Baisier, W.M., 1992. The kinetics of non-enzymatic browning. In: Schwartzberg, H.G., Hartel, R.W. (Eds.), Physical Chemistry of Foods. Marcel Dekker, Inc., New York, pp. 595–649 (chapter 14).

Lau, M., Tang, J., Taub, I., Yang, T., Edwards, C., Mao, R., 2003. Kinetics of chemical marker formation in whey protein gels for studying high temperature short time microwave sterilization. J. Food Eng. 60, 397–405.

Ledl, F., Schnell, W., Severin, T., 1995. Nachweis von 2,3-dihydro-3,5-dihydroxy-6-methyl-4H-pyran-4-on in lebensmitteln. Lebensm. Forschung 51 (17), 4947–4952.

Luan, D., Tang, J., Liu, F., Tang, Z., Li, F., Lin, H., Stewart, B., 2015a. Dielectric properties of bentonite water pastes used for stable loads in microwave thermal processing systems. J. Food Eng. 161, 40–47.

Luan, D., Tang, J., Pedrow, P.D., Liu, F., Tang, Z., 2015b. Performance of mobile metallic temperature sensors in high power microwave heating systems. J. Food Eng. 149, 114–122.

Martins, S.I., Jongen, W.M., Boekel, M.A.V., 2000. A review of Maillard reaction in food and implications to kinetic modelling. Trends Food Sci. Technol. 11 (9–10), 364–373.

Pandit, R., Tang, J., Liu, F., Mikhaylenko, G., 2007. A computer vision method to locate cold spots in foods in microwave sterilization processes. J. Pattern Recognit. Soc. 46 (12), 3667–3676.

Pandit, R., Tang, J., Mikhaylenko, G., Liu, F., 2006. Kinetics of chemical marker M-2 formation in mashed potato - a tool to locate cold spots under microwave sterilization. J. Food Eng. 76 (3), 353–361.

Peng, J., Tang, J., Barrett, D.M., Sablani, S.S., Powers, J.R., 2014. Kinetics of carrot texture degradation under pasteurization conditions. J. Food Eng. 122 (1), 84–91.

Ramaswamy, H., Awuah, G., Kim, H.-J., Choi, Y.-M., 1996. Evaluation of a chemical marker for process lethality measurement at 110 °C in a continuous flow holding tube. J. Food Process. Preserv. 20, 235–249.

Resurreccion, F., Tang, J., Pedrow, P., Cavalieri, R., Liu, F., Tang, Z., 2013. Development of a computer simulation model for processing food in a microwave assisted thermal sterilization (MATS) system. J. Food Eng. 118 (4), 406–416.

Resurreccion, F.P., 2012. Microwave Assisted Thermal Processing of Homogeneous and Heterogeneous Food Packed in a Polymeric Container. PhD thesis. Washington State University.

Ross, E.W., 1993. Relation of bacterial destruction to chemical marker formation during processing by thermal pulses. J. Food Process Eng. 16, 247–270.

Shaw, P.E., Tatum, J.H., Berry, R.E., 1968. Base-catalysed fructose degradation and its relation to nonenzymatic browning. J. Agric. Food Chem. 16 (6), 979–982.

Shaw, P.E., Tatum, J.H., Berry, R.E., 1971. 2,3-dihydro-3,5-dihydroxy-6-methyl-4H-pyran-4-one, a degradation product of a hexose. Carbohydr. Res. 16, 207–211.

Tang, J., 2015. Unlocking potentials of microwaves for food safety and quality. J. Food Sci. 80 (8), E1776–E1793.

Tang, J., Resurreccion, F.P., 2009. Electromagnetic basis of microwave heating. In: Lorence, M.W., Pescheck, P.S. (Eds.), Development of Packaging and Products for Use in Microwave Ovens, first ed. CRC press, Boca Raton, Florida, pp. 3–36.

Wang, Y., Lau, M.H., Tang, J., Mao, R., 2004. Kinetics of chemical marker M-1 formation in whey protein gels for developing sterilization processes based on dielectric heating. J. Food Eng. 64 (1), 111–118.

Wang, Y., Tang, J., Rasco, B., Kong, F., Wang, S., 2008. Dielectric properties of salmon fillets as a function of temperature and composition. J. Food Eng. 87 (2), 236–246.

Wang, Y., Wig, T.D., Tang, J., Hallberg, L.M., 2003. Dielectric properties of foods relevant to RF and microwave pasteurization and sterilization. J. Food Eng. 57, 257–268.

Zhang, W., Luan, D., Tang, J., Sablani, S.S., Rasco, B., Lin, H., Liu, F., 2015. Dielectric properties and other physical properties of low-acyl gellan gel as relevant to microwave assisted pasteurization process. J. Food Eng. 149, 195–203.

Zhang, W., Tang, J., Liu, F., Bohnet, S., Tang, Z., 2014. Chemical marker M2 (4-hydroxy-5-methyl-3(2H)-furanone) formation in egg white gel model for heating pattern determination of microwave-assisted pasteurization processing. J. Food Eng. 125, 69–76.